

Narrowband and ultranarrowband filters with electro-optic structurally chiral materials

Akhlesh Lakhtakia

*CATMAS — Computational & Theoretical Materials Sciences Group,
Department of Engineering Science & Mechanics,
Pennsylvania State University, University Park, PA 16802-6812, USA.
Tel: +1 814 863 4319; Fax: +1 814 865 9974; E-mail: akhlesh@psu.edu*

When a circularly polarized plane wave is normally incident on a slab of a structurally chiral material with local $\bar{4}2m$ point group symmetry and a central twist defect, the slab can function as either a narrowband reflection hole filter for co-handed plane waves or an ultranarrowband transmission hole filter for cross-handed plane waves, depending on its thickness and the magnitude of the applied dc electric field. Exploitation of the Pockels effect significantly reduces the thickness of the slab.

1 Introduction

Upon illumination by a normally incident, circularly polarized (CP) plane wave, a slab of a structurally chiral material (SCM) with its axis of nonhomogeneity aligned parallel to the thickness direction, is axially excited and reflects as well as transmits. Provided the SCM slab is periodically nonhomogeneous and sufficiently thick, and provided the wavelength of the incident plane wave lies in a certain wavelength regime, the circular Bragg phenomenon is exhibited. This phenomenon may be described as follows: reflection is very high if the handedness of the plane wave is the same as the structural handedness of the SCM, but is very low if the two handednesses are opposite of each other. This phenomenon has been widely used to make circular polarization filters of chiral liquid crystals [1] and chiral sculptured thin films [2]. If attenuation with the SCM slab is sufficiently low, it can thus function as a CP rejection filter. The circular Bragg phenomenon is robust enough that periodic perturbations of the basic helicoidal nonhomogeneity can be altered to obtain different polarization-rejection characteristics [3]–[6].

In general, structural defects in periodic materials produce localized modes of wave resonance either within the Bragg regime or at its edges. Narrowband CP filters have been fabricated by incorporating either a layer defect or a twist defect in the center of a SCM [2]. In the absence of the central defect, as stated earlier, co-handed CP light is substantially reflected in the Bragg regime while cross-handed CP light is not. The central defect creates a narrow transmission peak for co-handed CP light that pierces the Bragg regime, with the assumption that dissipation in the SCM slab is negligibly small.

Numerical simulations show that, as the total thickness of a SCM slab with a central defect increases, the bandwidth of the narrow transmission peak begins to diminish and an even narrower peak begins to develop in the reflection spectrum of the cross-handed CP plane wave. There is a crossover thickness of the device at which the two peaks are roughly equal in intensity. Further increase in device thickness causes the co-handed transmission peak to diminish more and eventually vanish, while the cross-handed reflection peak gains its full intensity and then saturates [7], [8]. The bandwidth of the cross-handed reflection peak is a small fraction of that of the co-handed transmission peak displaced by it. Such a crossover phenomenon cannot be exhibited by the commonplace scalar Bragg gratings, and is unique to periodic SCMs [8]. An explanation for the crossover phenomenon has recently been provided in terms of coupled wave theory [9].

Although the co-handed transmission peak (equivalently, reflection hole) has been observed and even utilized for both sensing [10] and lasing [11], the cross-handed reflection peak (or transmission hole) remains entirely a theoretical construct. The simple reason is that the total thickness for crossover is very large [7]–[9]. Even a small amount of dissipation evidently vitiates the conditions for the emergence of cross-handed reflection peak. Clearly, if the crossover thickness could be significantly reduced, the chances for the development of the cross-handed reflection peak would be greatly enhanced.

Such a reduction could be possible if the SCM were to display the Pockels effect [12] — this thought emerged as a result of establishing the effect of a dc electric field on a defect-free SCM endowed with a local $\bar{4}2m$ point group symmetry [13]. A detailed investigation, as reported in the following sections, turned out to validate the initial idea.

The plan of this paper is as follows: Section 2 contains a description of the boundary value problem when a CP plane wave is normally incident on a SCM slab with local $\bar{4}2m$ point group symmetry and a central twist defect. Section 3 contains sample numerical results to demonstrate that the chosen device can function as either a narrowband reflection hole filter or an ultranarrowband transmission hole filter — depending on (i) the thickness of the SCM slab, (ii) the handedness of the incident plane wave, and (iii) the magnitude of the applied dc electric field. Vectors are denoted in boldface; the cartesian unit vectors are represented by $\hat{\mathbf{u}}_x$, $\hat{\mathbf{u}}_y$, and $\hat{\mathbf{u}}_z$; symbols for column vectors and matrixes are decorated by an overbar; and an $\exp(-i\omega t)$ time-dependence is implicit with ω as the angular frequency. The wavenumber and the intrinsic impedance of free space are denoted by $k_0 = \omega\sqrt{\epsilon_0\mu_0}$ and $\eta_0 = \sqrt{\mu_0/\epsilon_0}$, respectively, with μ_0 and ϵ_0 being the permeability and permittivity of free space.

2 Boundary Value Problem

Suppose that a SCM slab with a central twist defect occupies the region $0 \leq z \leq 2L$, the halfspaces $z \leq 0$ and $z \geq 2L$ being vacuous. An arbitrarily polarized plane wave is normally incident on the device from the halfspace $z \leq 0$. In consequence, a reflected plane wave also exists in the same halfspace and a transmitted plane wave in the halfspace $z \geq 2L$.

The total electric field phasor in the halfspace $z \leq 0$ is given by

$$\mathbf{E}(\mathbf{r}) = (a_L \hat{\mathbf{u}}_+ + a_R \hat{\mathbf{u}}_-) \exp(ik_0 z) + (r_L \hat{\mathbf{u}}_- + r_R \hat{\mathbf{u}}_+) \exp(-ik_0 z), \quad z \leq 0, \quad (1)$$

where $\mathbf{u}_\pm = (\hat{\mathbf{u}}_x \pm i\hat{\mathbf{u}}_y)/\sqrt{2}$. Likewise, the electric field phasor in the halfspace $z \geq 2L$ is represented as

$$\mathbf{E}(\mathbf{r}) = (t_L \hat{\mathbf{u}}_+ + t_R \hat{\mathbf{u}}_-) \exp[ik_0(z - 2L)], \quad z \geq 2L. \quad (2)$$

Here, a_L and a_R are the known amplitudes of the left- and the right-CP (LCP & RCP) components of the incident plane wave; r_L and r_R are the unknown amplitudes of the reflected plane wave components; while t_L and t_R are the unknown amplitudes of the transmitted plane wave components. The aim in solving the boundary value problem is to determine $r_{L,R}$ and $t_{L,R}$ for known a_L and a_R .

2.1 Electro-optic SCM with Local $\bar{4}2m$ Symmetry

The chosen electro-optic SCM slab has the z axis as its axis of chiral nonhomogeneity, and is subject to a dc electric field $\mathbf{E}^{dc} = E_z^{dc} \hat{\mathbf{u}}_z$. The slab is assumed to have a local $\bar{4}2m$ point group symmetry.

The optical relative permittivity matrix in the region $0 < z < 2L$ may be stated as follows [13]:

$$\begin{aligned} \bar{\epsilon}^{SCM}(z) &= \bar{S}_z \left[h \frac{\pi z}{\Omega} + h\psi(z) \right] \cdot \bar{R}_y(\chi) \\ &\cdot \begin{pmatrix} \epsilon_1^{(0)} & -r_{63} \epsilon_1^{(0)2} E_z^{dc} \sin \chi & 0 \\ -r_{63} \epsilon_1^{(0)2} E_z^{dc} \sin \chi & \epsilon_1^{(0)} & -r_{41} \epsilon_1^{(0)} \epsilon_3^{(0)} E_z^{dc} \cos \chi \\ 0 & -r_{41} \epsilon_1^{(0)} \epsilon_3^{(0)} E_z^{dc} \cos \chi & \epsilon_3^{(0)} \end{pmatrix} \\ &\cdot \bar{R}_y(\chi) \cdot \bar{S}_z^{-1} \left[h \frac{\pi z}{\Omega} + h\psi(z) \right], \quad 0 < z < 2L. \end{aligned} \quad (3)$$

Whereas $\epsilon_1^{(0)}$ and $\epsilon_3^{(0)}$ are, respectively, the squares of the ordinary and the extraordinary refractive indexes in the absence of the Pockels effect, r_{41} and r_{63} are the electro-optic coefficients relevant to the $\bar{4}2m$ point group symmetry [12]; and only the lowest-order approximation of the Pockels effect has been retained on the right side of $\bar{\epsilon}$. The tilt matrix

$$\bar{R}_y(\chi) = \begin{pmatrix} -\sin \chi & 0 & \cos \chi \\ 0 & -1 & 0 \\ \cos \chi & 0 & \sin \chi \end{pmatrix} \quad (4)$$

involves the angle $\chi \in [0, \pi/2]$ with respect to the x axis in the xz plane. The use of the rotation matrix

$$\bar{S}_z(\zeta) = \begin{pmatrix} \cos \zeta & -\sin \zeta & 0 \\ \sin \zeta & \cos \zeta & 0 \\ 0 & 0 & 1 \end{pmatrix} \quad (5)$$

in $\bar{\epsilon}$ involves the half-pitch Ω of the SCM along the z axis. In addition, the handedness parameter $h = 1$ for structural right-handedness and $h = -1$ for structural left-handedness.

The angle $\psi(z)$ helps delineate the central twist as follows:

$$\psi(z) = \begin{cases} 0, & 0 < z < L \\ \Psi, & L < z < 2L. \end{cases} \quad (6)$$

The angle $\Psi \in [0, \pi]$ is a measure of the central twist defect.

2.2 Reflectances and Transmittances

The procedure to obtain the unknown reflection and transmission amplitudes involves the 4×4 matrix relation [2]

$$\bar{f}_{exit} = \bar{M} \cdot \bar{f}_{entry}, \quad (7)$$

where the column 4-vectors

$$\bar{f}_{entry} = \frac{1}{\sqrt{2}} \begin{pmatrix} (r_L + r_R) + (a_L + a_R) \\ i [-(r_L - r_R) + (a_L - a_R)] \\ -i [(r_L - r_R) + (a_L - a_R)] / \eta_0 \\ -[(r_L + r_R) - (a_L + a_R)] / \eta_0 \end{pmatrix} \quad (8)$$

and

$$\bar{f}_{exit} = \frac{1}{\sqrt{2}} \begin{pmatrix} t_L + t_R \\ i (t_L - t_R) \\ -i (t_L - t_R) / \eta_0 \\ (t_L + t_R) / \eta_0 \end{pmatrix} \quad (9)$$

denote the electromagnetic fields at the entry and the exit pupils, respectively. The 4×4 matrix

$$\bar{M} = \bar{B}(h\Psi) \cdot \left[\bar{B} \left(h \frac{\pi L}{\Omega} \right) \cdot \exp(i\bar{A}'L) \right] \cdot \bar{B}(-h\Psi) \cdot \left[\bar{B} \left(h \frac{\pi L}{\Omega} \right) \cdot \exp(i\bar{A}'L) \right], \quad (10)$$

where

$$\bar{A}' = \begin{pmatrix} 0 & -\frac{ih\pi}{\Omega} & 0 & \omega\mu_0 \\ \frac{ih\pi}{\Omega} & 0 & -\omega\mu_0 & 0 \\ -\omega\epsilon_0\epsilon_e & -\omega\epsilon_0\epsilon_e^{(0)} & 0 & -\frac{ih\pi}{\Omega} \\ \omega\epsilon_0\epsilon_d & \omega\epsilon_0\epsilon_e & \frac{ih\pi}{\Omega} & 0 \end{pmatrix}, \quad (11)$$

$$\bar{B}(\zeta) = \begin{pmatrix} \cos\zeta & -\sin\zeta & 0 & 0 \\ \sin\zeta & \cos\zeta & 0 & 0 \\ 0 & 0 & \cos\zeta & -\sin\zeta \\ 0 & 0 & \sin\zeta & \cos\zeta \end{pmatrix}, \quad (12)$$

$$\epsilon_d = \frac{\epsilon_1^{(0)}\epsilon_3^{(0)}}{\epsilon_1^{(0)}\cos^2\chi + \epsilon_3^{(0)}\sin^2\chi}, \quad (13)$$

and

$$\epsilon_e = E_z^{dc}\epsilon_1^{(0)}\epsilon_d(r_{41}\cos^2\chi - r_{63}\sin^2\chi). \quad (14)$$

The foregoing expression for \bar{A}' is correct to the lowest order in both $r_{41}E_z^{dc}$ and $r_{63}E_z^{dc}$.

The reflection amplitudes $r_{L,R}$ and the transmission amplitudes $t_{L,R}$ can be computed for specified incident amplitudes (a_L and a_R) by solving eq8. Interest usually lies in determining the reflection and transmission coefficients entering the 2×2 matrixes in the following two relations:

$$\begin{pmatrix} r_L \\ r_R \end{pmatrix} = \begin{pmatrix} r_{LL} & r_{LR} \\ r_{RL} & r_{RR} \end{pmatrix} \begin{pmatrix} a_L \\ a_R \end{pmatrix}, \quad (15)$$

$$\begin{pmatrix} t_L \\ t_R \end{pmatrix} = \begin{pmatrix} t_{LL} & t_{LR} \\ t_{RL} & t_{RR} \end{pmatrix} \begin{pmatrix} a_L \\ a_R \end{pmatrix}. \quad (16)$$

Both 2×2 matrixes are defined phenomenologically. The co-polarized transmission coefficients are denoted by t_{LL} and t_{RR} , and the cross-polarized ones by t_{LR} and t_{RL} ; and similarly for the reflection coefficients in eq15. Reflectances and transmittances are denoted, e.g., as $T_{LR} = |t_{LR}|^2$.

3 Numerical Results

Calculations of the reflectances and transmittances as functions of the parameter λ_0/Ω were made with and without electro-optic properties. The constitutive parameters used are that of ammonium dihydrogen phosphate at $\lambda_0 = 546$ nm [12], [14]: $\epsilon_1^{(0)} = 1.53^2$, $\epsilon_3^{(0)} = 1.483^2$, $r_{41} = 24.5 \times 10^{-12}$ m V $^{-1}$ and $r_{63} = 8.5 \times 10^{-12}$ m V $^{-1}$. For illustrative results, the SCM was chosen to be structurally right-handed (i.e., $h = 1$) and the tilt angle χ was fixed at $\pi/6$. The parameter L/Ω was constrained to be an even integer.

Figures 1 and 2 present the variations of the reflectances and transmittances with the normalized wavelength λ_0/Ω when the Pockels effect is not invoked (i.e., $E_z^{dc} = 0$), for $L = 30\Omega$ and $L = 180\Omega$, respectively. The twist defect $\Psi = \pi/2$. A co-handed reflection hole is clearly evident in the plot of R_{RR} at $\lambda_0/\Omega \simeq 3.02$, and the corresponding co-handed transmission peak may be seen in the plot of T_{RR} in Figure 1. This hole/peak-feature is of high quality. As the ratio L/Ω was increased, this

feature began to diminish and was replaced by a cross-handed transmission hole in the plot of T_{LL} along with a corresponding cross-handed peak in the plot of R_{LL} . At $L = 180\Omega$ (Figure 2), the second feature is of similar quality to the feature in Figure 1. The bandwidth of the second feature is a tiny fraction of the first feature, however. Neither of the two features requires further discussion, as their distinctive features are known well [7], [9], [15], [16], except to note that they constitute a defect mode of propagation along the axis of chiral nonhomogeneity.

Figures 3 and 4 are the analogs of Figures 1 and 2, respectively, when the Pockels effect has been invoked by setting $E_z^{dc} = 1.5 \text{ GV m}^{-1}$. Although $L = 16\Omega$ in Figure 3, the narrowband feature therein is of the same high quality as in Figure 1. The ultranarrowband feature for $L = 58\Omega$ in Figure 4 is wider than its counterpart in Figure 2, but could still be acceptable for many purposes. The inevitable conclusion is that the incorporation of the Pockels effect in suitable SCMs provides a means to realize thinner narrowband and ultranarrowband filters that are also CP-discriminatory. This is the main result of this communication.

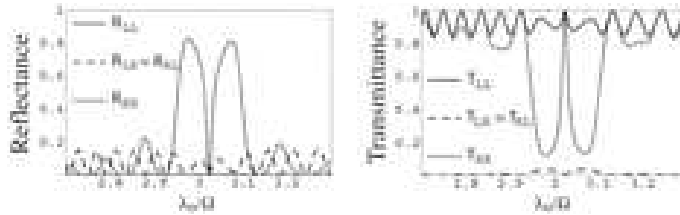


Figure 1: Reflectances (R_{LL} , etc.) and transmittances (T_{LL} , etc.) as functions of the normalized wavelength λ_0/Ω , when $L = 30\Omega$, $\Psi = 90^\circ$, and $E_z^{dc} = 0$. The other parameters are: $\epsilon_1^{(0)} = 1.53^2$, $\epsilon_3^{(0)} = 1.483^2$, $r_{41} = 24.5 \times 10^{-12} \text{ m V}^{-1}$, $r_{63} = 8.5 \times 10^{-12} \text{ m V}^{-1}$, $h = 1$, and $\chi = 30^\circ$.

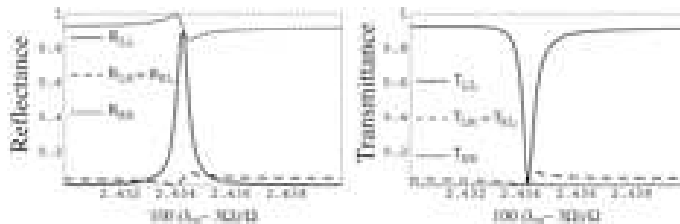


Figure 2: Same as Figure 1, except that $L = 180\Omega$.

An examination of the eigenvalues of \bar{A}' shows that the Bragg regime of the defect-free SCM is delineated by [13]

$$\lambda_{0_{min}} \leq \lambda_0 \leq \lambda_{0_{max}}, \quad (17)$$

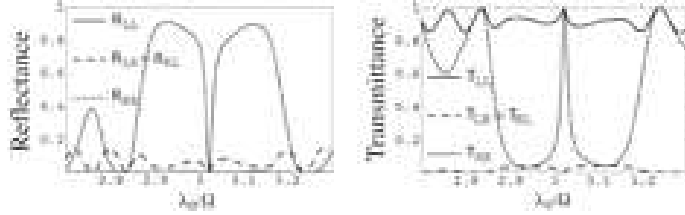


Figure 3: Same as Figure 1, except that $L = 16\Omega$ and $E_z^{dc} = 1.5 \times 10^9 \text{ V m}^{-1}$.



Figure 4: Same as Figure 2, except that $L = 58\Omega$ and $E_z^{dc} = 1.5 \times 10^9 \text{ V m}^{-1}$.

where

$$\lambda_{0_{min}} = 2\Omega \min \{ \sqrt{\epsilon_{1\varphi}}, \sqrt{\epsilon_{d\varphi}} \}, \quad (18)$$

$$\lambda_{0_{max}} = 2\Omega \max \{ \sqrt{\epsilon_{1\varphi}}, \sqrt{\epsilon_{d\varphi}} \}, \quad (19)$$

$$\epsilon_{1\varphi} = \frac{1}{2} \left[\epsilon_1^{(0)} + \epsilon_d + \frac{(\epsilon_1^{(0)} - \epsilon_d)^2 + 4\epsilon_e^2}{\epsilon_1^{(0)} - \epsilon_d} \cos 2\varphi \right], \quad (20)$$

$$\epsilon_{d\varphi} = \frac{1}{2} \left[\epsilon_1^{(0)} + \epsilon_d - \frac{(\epsilon_1^{(0)} - \epsilon_d)^2 + 4\epsilon_e^2}{\epsilon_1^{(0)} - \epsilon_d} \cos 2\varphi \right], \quad (21)$$

and

$$\varphi = \frac{1}{2} \tan^{-1} \left(\frac{2h\epsilon_e}{\epsilon_d - \epsilon_1^{(0)}} \right). \quad (22)$$

Depending on the values of the constitutive parameters, the introduction of E_z^{dc} enhances the difference $|\sqrt{\epsilon_{d\varphi}} - \sqrt{\epsilon_{1\varphi}}|$ significantly either for $\chi < \tan^{-1} \sqrt{r_{41}/r_{63}}$ or $\chi > \tan^{-1} \sqrt{r_{41}/r_{63}}$. For the parameters selected for Figures 1–4, this enhancement is significant for low values of χ . The greater the enhancement, the faster does the circular Bragg phenomenon develop as the normalized thickness L/Ω is increased [2]. No wonder, the two types of spectral holes appear for smaller values of L/Ω when E_z^{dc} is switched on.

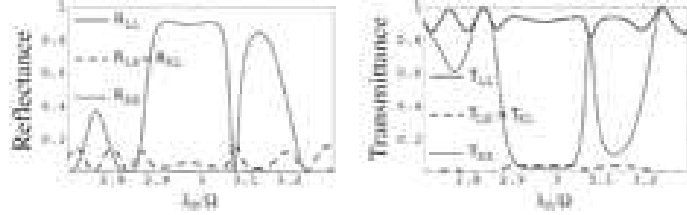


Figure 5: Reflectances (R_{LL} , etc.) and transmittances (T_{LL} , etc.) as functions of the normalized wavelength λ_0/Ω , when $L = 16\Omega$, $\Psi = 60^\circ$, and $E_z^{dc} = 1.5 \times 10^9 \text{ V m}^{-1}$. The other parameters are: $\epsilon_1^{(0)} = 1.53^2$, $\epsilon_3^{(0)} = 1.483^2$, $r_{41} = 24.5 \times 10^{-12} \text{ m V}^{-1}$, $r_{63} = 8.5 \times 10^{-12} \text{ m V}^{-1}$, $h = 1$, and $\chi = 30^\circ$.

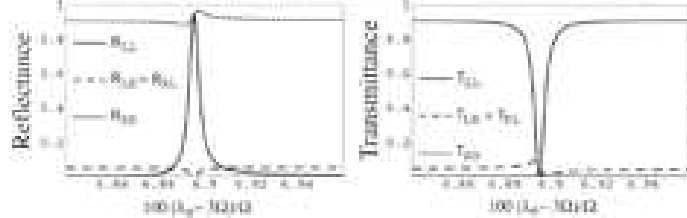


Figure 6: Same as Figure 5, except that $L = 70\Omega$.

Both types of spectral holes for $\Psi = \pi/2$ are positioned approximately in the center of the wavelength regime Br -range, which is the Bragg regime of a defect-free SCM [13]. For other values of Ψ , the locations of the spectral holes may be estimated as [9], [15]

$$\lambda_0 = \frac{1}{2} [\lambda_{0_{min}} + \lambda_{0_{max}} + (\lambda_{0_{max}} - \lambda_{0_{min}}) \cos \Psi] . \quad (23)$$

Figures 5 and 6 present sample results for $\Psi = \pi/3$ in support. However, let it be noted that the location of the spectral holes can be manipulated simply by changing Ω while fixing $\Psi = \pi/2$.

4 Concluding Remarks

The boundary value problem presented in this paper is of the reflection and transmission of a circularly polarized plane wave that is normally incident on a slab of a structurally chiral material with local $\bar{4}2m$ point group symmetry and a central twist defect. Numerical results show that the slab can function as either a narrowband reflection hole filter for co-handed CP plane waves or an ultranarrowband transmission hole filter for cross-handed CP plane waves, depending on its thickness and the magnitude of the applied dc electric field. Exploitation of the Pockels effect significantly reduces the thickness of the slab for adequate performance. The presented results are expected to urge experimentalists to fabricate, characterize, and optimize the proposed devices.

This paper is affectionately dedicated to Prof. R. S. Sirohi on the occasion of his retirement as the Director of the Indian Institute of Technology, New Delhi.

References

1. Jacobs S D (ed), *Selected papers on liquid crystals for optics*. (SPIE Optical Engineering Press,

Bellingham, WA, USA), 1992.

- 2. Lakhtakia A, Messier R, *Sculptured thin films: Nanoengineered morphology and optics.* (SPIE Press, Bellingham, WA, USA), 2005, Chap. 10.
- 3. Polo Jr J A, Lakhtakia A, *Opt. Commun.* 242 (2004) 13.
- 4. Polo Jr J A, *Electromagnetics* 25 (2005) 409.
- 5. Hodgkinson I, Wu Q h, De Silva L, Arnold M, Lakhtakia A, McCall M, *Opt. Lett.* 30 (2005) 2629.
- 6. Ross B M, Lakhtakia A, Hodgkinson I J, *Opt. Commun.* (doi:10.1016/j.optcom.2005.09.051).
- 7. Kopp V I, Genack A Z, *Phys. Rev. Lett.* 89 (2002) 033901.
- 8. Wang F, Lakhtakia A, *Opt. Commun.* 215 (2003) 79.
- 9. Wang F, Lakhtakia A, *Proc. R. Soc. Lond. A* 461 (2005) 2985.
- 10. Lakhtakia A, McCall M W, Sherwin J A, Wu Q H, Hodgkinson I J, *Opt. Commun.* 194 (2002) 33.
- 11. Schmidtke J, Stille W, Finkelmann H, *Phys. Rev. Lett.* 90 (2003) 083902.
- 12. Boyd R W, *Nonlinear optics.* (Academic Press, London, UK), 1992, Chap. 10.
- 13. Reyes J A, Lakhtakia A, *Opt. Commun.* (doi:10.1016/j.optcom.2005.08.034).
- 14. http://www.kayelaby.npl.co.uk/general_physics/2_5/2_5_8.html
- 15. Schmidtke J, Stille W, *Eur. Phys. J. E* 12 (2003) 553.
- 16. Wang F, Lakhtakia A, *Opt. Exp.* 13 (2005) 7319.